Neuron, Vol. 31, 131–141, July 19, 2001, Copyright ©2001 by Cell Press

Timing and Location of Nicotinic Activity Enhances or Depresses Hippocampal Synaptic Plasticity

Daoyun Ji, Remigijus Lape, and John A. Dani[1]
Division of Neuroscience and
Structural and Computational Biology
and Molecular Biophysics Program
Baylor College of Medicine
One Baylor Plaza
Houston, Texas 77030

Summary

This study reveals mechanisms in the mouse hippocampus that may underlie nicotinic influences on attention, memory, and cognition. Induction of synaptic plasticity, arising via generally accepted mechanisms, is modulated by nicotinic acetylcholine receptors. Properly timed nicotinic activity at pyramidal neurons boosted the induction of long-term potentiation via presynaptic and postsynaptic pathways. On the other hand, nicotinic activity on interneurons inhibited nearby pyramidal neurons and thereby prevented or diminished the induction of synaptic potentiation. The synaptic modulation was dependent on the location and timing of the nicotinic activity. Loss of these synaptic mechanisms may contribute to the cognitive deficits experienced during Alzheimer's diseases, which is associated with a loss of cholinergic projections and with a decrease in the number of nicotinic receptors.

Introduction

Studies using agonists, antagonists, and specific cholinergic lesions have shown that nicotinic cholinergic systems contribute to attention, learning, and working memory in rodents, nonhuman primates, and humans (Jones et al., 1999; Levin and Simon, 1998; Newhouse et al., 1997). The impact of the various experimental manipulations is task specific. For example, nicotinic agonists do not improve reference memory, but they often improve working memory in tasks such as passive avoidance (Brioni and Arneric, 1993) and delayed match to sample (Buccafusco et al., 1995). It is often found that nicotinic manipulations have the greatest impact on difficult tasks or on cognitively impaired subjects (Levin and Simon, 1998). A good example is Alzheimer's disease, which is accompanied by a reduction of cholinergic projections and loss of nicotinic receptors in the cortex and hippocampus (Paterson and Nordberg, 2000). Nicotine skin patches can improve learning rates and attention in those patients, and inhibition of acetylcholinesterase is the most accepted treatment (Levin and Rezvani, 2000).

Some of the influence of nicotinic agents is linked to the hippocampus, an important structure for learning and memory. Local infusion of nicotinic antagonists impairs memory performance (Ohno et al., 1993), and nicotine reverses working memory deficits produced by lesioning cholinergic projections to the hippocampus (Grigoryan et al., 1994). These findings are consistent with the hippocampus having dense expression of nicotinic acetylcholine receptors (nAChRs) (Wada et al., 1989; Séguéla et al., 1993) and having abundant cholinergic innervation mainly from the medial septum-diagonal band complex (Woolf, 1991). A fine network of cholinergic fibers is found throughout the hippocampus and fascia dentata, and synaptic contacts are made onto pyramidal cells, granule cells, interneurons, and neurons of the hilus (Frotscher and Leranth, 1985). These anatomical findings are reinforced by the discovery of fast nicotinic transmission onto interneurons and pyramidal neurons (Alkondon et al., 1998; Frazier et al., 1998a; Hefft et al., 1999; Jones et al., 1999). In addition to those direct cholinergic synaptic connections, there also is evidence for significant nonsynaptic, volume transmission for ACh in the hippocampus (Umbriaco et al., 1995).

The accumulation of evidence indicates that synaptic plasticity, such as short-term potentiation (STP) and long-term potentiation (LTP), participates during the learning and memory process (Martin et al., 2000). LTP has been extensively studied in the CA1 region of the hippocampus, where NMDA receptor activity initiates a calcium-dependent transduction cascade that produces the synaptic change (Malenka and Nicoll, 1999). Inhibitory GABAergic interneurons can modulate the induction of synaptic plasticity by shunting the incoming excitatory drive (Staley and Mody, 1992).

Bath applied nicotine or long in vivo exposure to nicotine is capable of altering hippocampal synaptic plasticity (Fujii et al., 1999; Hamid et al., 1997). In an elegant study, Mansvelder and McGehee (2000) showed that the coincidence of presynaptic nAChR activity and postsynaptic depolarization produced LTP of glutamatergic cortical afferents into the ventral tegmental area. That result is consistent with many studies showing that presynaptic nAChRs can enhance the release of neurotransmitters (Albuquerque et al., 1997; Alkondon et al., 1996; Aramakis and Metherate, 1998; Coggan et al., 1997; Girod et al., 2000; Lena and Changeux, 1997; McGehee et al., 1995; McGehee and Role, 1995; Wonnacott, 1997), including glutamate and GABA in the hippocampus (Alkondon et al., 1997a; Gray et al., 1996; Radcliffe and Dani, 1998). In this study of mouse hippocampal slices, we show that nAChR activity can enhance or depress synaptic plasticity, and the form of the modulation depends on the location and timing of the nAChR activity. Further, we address an area of some controversy (Frazier et al., 1998b; Hefft et al., 1999; Jones and Yakel, 1997; McQuiston and Madison, 1999) by showing that nAChRs are located on pyramidal neurons as well as interneurons.

Results

Nicotinic Currents from CA1 Pyramidal Neurons

There is some ambiguity regarding nAChR expression and nicotinic currents in pyramidal neurons. To address

[1] Correspondence: jdani@bcm.tmc.edu

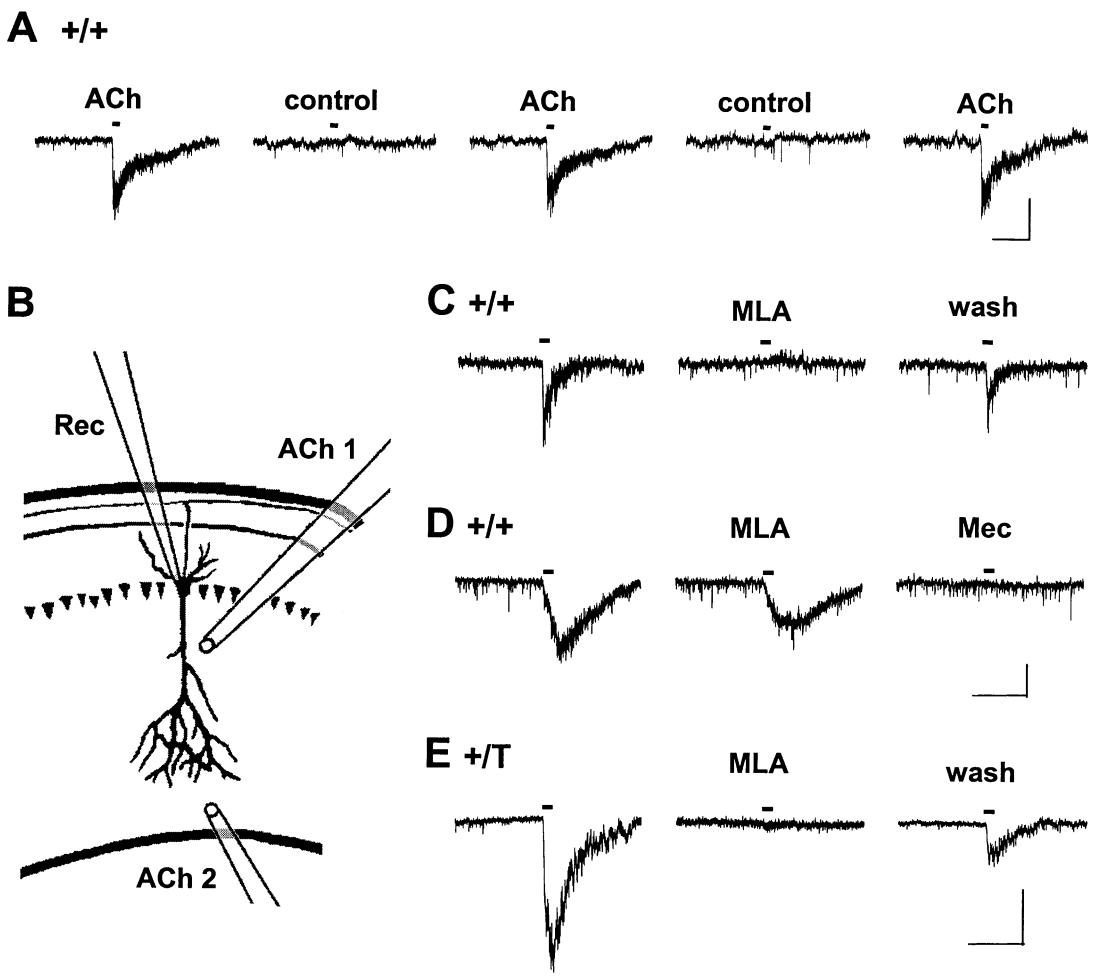

Figure 1. ACh-Induced Nicotinic Currents from CA1 Pyramidal Neurons

(A) Pressure injection via a puffer pipette induces nAChRs current when the pipette contains 1 mM ACh (solid bar, ACh), but there is not detectable current when the puffer injects bath solution as a control (solid bar, control). The 1 s puffs were separated by 20 s, and three puffs of ACh were followed by three puffs of control solution. This process continued for 20 min (n = 6). The scale bars represents 5 s and 10 pA. All of the traces in this figure are the average of three adjacent records.

(B) Didactic diagram showing a pyramidal neuron that was voltage clamped to record (Rec) the nicotinic currents. A puffer pipette located roughly perpendicular to the proximal dendrites (ACh 1) produces smaller nAChR currents than a puffer pipette aimed more parallel to the distal dendrites (ACh 2).

(C) The ACh puffs (solid bars) activated nicotinic currents that were inhibited by the α7 specific inhibitor, 20 nM MLA. The recordings were from a (+/+) wild-type mouse. The scale bars in (D) apply.

(D) The ACh puffs (solid bars) activated nicotinic currents that were not completely inhibited by MLA, but they were inhibited by the nonspecific nAChR inhibitor, 20 μM mecamylamine (Mec). The recordings were from a (+/+) wild-type mouse. The scale bars represent 5 s and 20 pA.

(E) In heterozygous mutant mice containing the α7 L250T mutation (+/T), the ACh puff (solid bar) activated a larger current. The nicotinic currents were completely inhibited by 20 nM MLA, indicating α7 nAChRs. The scale bars represent 5 s and 50 pA.

that issue, we recorded ACh-induced nicotinic currents from CA1 pyramidal neurons. Muscarinic receptors were inhibited with atropine in all of the experiments. First, we verified that local, rapid pressure applications via a puffer pipette did not produce artifacts. Two identical puffer pipettes were placed next to each other near the distal dendrites. One puffer pipette contained 1 mM ACh and the other contained bath solution as a control. Alternate puffer applications were applied, and under our conditions, the ACh puffer activated a current and the control puffer did not (Figure 1A).

To activate nAChR currents, we used two different positions of the ACh puffer pipette (Figure 1B). Puffs of ACh in the proximal dendrites roughly perpendicular to the arbor produced small currents in CA1 pyramidal neurons (ACh 1; Figure 1B). In a third of the trials, the nAChR currents were easily measured as larger than 5 pA, with an average current of 11.9 $\pm$ 2.9 pA, n = 12 out of 35. Puffs of ACh in the distal dendrites roughly parallel to the arbor produced larger currents (ACh 2; Figure 1B). In 90% of the trials, the currents were larger than 5 pA, with an average of 25.5 $\pm$ 1.2 pA, n = 134 out of 149. In 9 out of 11 trials, the nicotinic currents were inhibited by methyllycaconitine (MLA), a specific inhibitor of α7* nAChRs (Figure 1C). However, other nAChR subtypes were present more rarely or as a minor-

ity component, and those currents were blocked by the nonspecific nicotinic inhibitor, mecamylamine (Figure 1D).

It was often the case that the ACh-induced currents were small because our pressure applications of ACh were only hitting a relatively small area of the pyramidal neurons. To verify our estimate of ACh-responding CA1 neurons, we took advantage of heterozygote mutant mice (+/T), having one copy of the α7 subunit with a leucine to threonine mutation (L250T) (Orr-Urtreger et al., 2000). This mutation causes the α7* currents to be larger (Revah et al., 1991; Bertrand et al., 1992). When the puffer pipette was in position 1 (ACh 1; Figure 1B), more than 90% of the CA1 pyramidal neurons tested from heterozygote L250T mice displayed nAChR currents larger than 5 pA, with an average current of 43.7 $\pm$ 5.3 pA, n = 30 out of 33. When the puffer pipette was in position 2 (ACh 2; Figure 1B), 100% of the CA1 pyramidal neurons displayed nAChR currents larger than 5 pA, with an average current of 126.7 $\pm$ 18.5 pA, n = 18 (Figure 1E). When measurable, the ACh-induced currents were about four times larger in the mutant (+/T) mice than in their wild-type (+/+) littermates. In 7 out of 9 trials with the mutant mice, MLA inhibited the nicotinic currents (Figure 1E), indicating α7* nAChRs carry most, but not necessarily all, of the nicotinic current from CA1 pyramidal neurons.

STP Boosted to LTP by Nicotinic Receptors on Pyramidal Neurons

We next determined whether nAChR activity on CA1 pyramidal neurons could affect synaptic plasticity. While recording from a CA1 pyramidal neuron, the Schaffer collateral pathway in the stratum radiatum was electrically stimulated to induce STP reliably, using the following protocol: 100 Hz for 1 s paired with a 100 pA depolarizing current applied to the postsynaptic CA1 pyramidal neuron. The test evoked postsynaptic potentials (ePSPs) that were no longer significantly larger than baseline ($p > 0.05$) 19 min after the stimulation for +/+ mice (Figure 2A; n = 7) and 16 min after the stimulation for +/T mice (Figure 2B; n = 8). With this paradigm of electrical stimulation applied to the +/+ mice, 6 of the 7 cells tested underwent STP and 1 underwent LTP. With the +/T mice, 6 of the 8 cells underwent STP and 2 underwent LTP.

In separate experiments, this same Schaffer collateral electrical stimulation was paired with postsynaptic nAChR currents induced by an ACh-puffer pipette (Figure 2C). To determine exactly when the Schaffer collateral stimulation should be applied, we first voltage clamped the CA1 pyramidal neuron and measured the amplitude and time of the postsynaptic nicotinic current induced by the ACh puffer (Figures 2D and 2E, inset). We selected pyramidal neurons with relatively large postsynaptic currents (>30 pA). Knowing the timing, the computer was set to apply Schaffer collateral stimulation just prior to the peak of the ACh-induced nicotinic current, as indicated by the arrow below the insert of Figures 2D and 2E. The pyramidal cell recording was then changed to current clamp, and the induction paradigm was applied. Regardless of the genotype of the mouse, when the electrical stimulation was paired with ACh-induced currents that were >30 pA, exactly the same paradigm that produced STP previously (Figures 2A and 2B), produced LTP (Figure 2D and 2E). When the electrical stimulation was paired with nAChR activity, the test ePSPs were significantly larger than baseline for as long as the experiments lasted. With this paradigm of electrical and ACh stimulation applied to the +/+ mice, 10 of the 14 cells tested underwent LTP and 4 underwent longer-lasting STP. With the +/T mice, 7 of the 9 slices underwent LTP and 2 underwent longer-lasting STP. It should be noted that it was easier to find cells from +/T mice that produced ACh-induced currents that were larger than 30 pA.

To verify that postsynaptic nicotinic currents were the cause of the switch from STP to LTP, we conducted the same pairing of ACh puffs with electrical stimulation, but selected neurons with small postsynaptic nAChR currents (<10 pA). When the pyramidal neurons responded with small postsynaptic nAChR currents, pairing ACh application with the identical electrical stimulation did not significantly change the STP (Figure 2F). Under these conditions, the test ePSPs were no longer significantly larger than baseline ($p > 0.05$) after 18 min. Of the 7 cells tested, 6 underwent STP and 1 underwent LTP.

Another issue to consider is that miniature excitatory postsynaptic currents (mEPSCs) occasionally accompanied the application of ACh (Figure 3), likely arising from enhanced glutamate release owing to presynaptic nAChR activity. We examined the mEPSCs because the ACh-induced release of glutamate coupled with a postsynaptic depolarization can cause synaptic potentiation (Mansvelder and McGehee, 2000). In TTX to block action potentials, 7 of 24 cells from wild-type mice showed an increased frequency of mEPSCs (Figures 3A and 3B). The ACh puff (1 mM for 1 s) elevated the mEPSC frequency for about 30 s (Figure 3C) but did not alter the mEPSC amplitude (Figure 3D). Ionotropic glutamate receptor inhibitors (CNQX and AP-5) blocked the mEPSCs. ACh puffs did not increase the mEPSC frequency when Mg^{2+} replaced Ca^{2+} in the bath solution (n = 5). These findings are consistent with the activity of presynaptic nAChRs.

We tested whether the increased presynaptic release of glutamate had a dominant effect in the ACh-induced boost of STP to LTP (Figure 2). We paired the puff of ACh with a postsynaptic depolarization (100 pA injected as before), but the presynaptic electrical stimulation was not applied. On average (n = 7), the ACh puff coupled to postsynaptic depolarization was not sufficient to induce any change in the test eEPSC (Figure 4A). In 6 of the 7 cells, the paradigm produced no effect, but in 1 cell LTP was produced. A similar paradigm applied in the ventral tegmental area by Mansvelder and McGehee (2000) had a higher probability of success.

The final test was to determine whether the electrical stimulation with a stronger postsynaptic depolarization, but without an ACh puff, would produce consistent LTP. The same electrical stimulation applied to the Schaffer collaterals in Figure 2 (100 Hz for 1 s) was paired with a postsynaptic depolarization that was twice as large. The current injected postsynaptically was doubled from 100 pA to 200 pA, but no ACh was applied. On average, the STP lasted longer (significant to 30 min), but LTP was not consistently produced (Figure 4B). With this

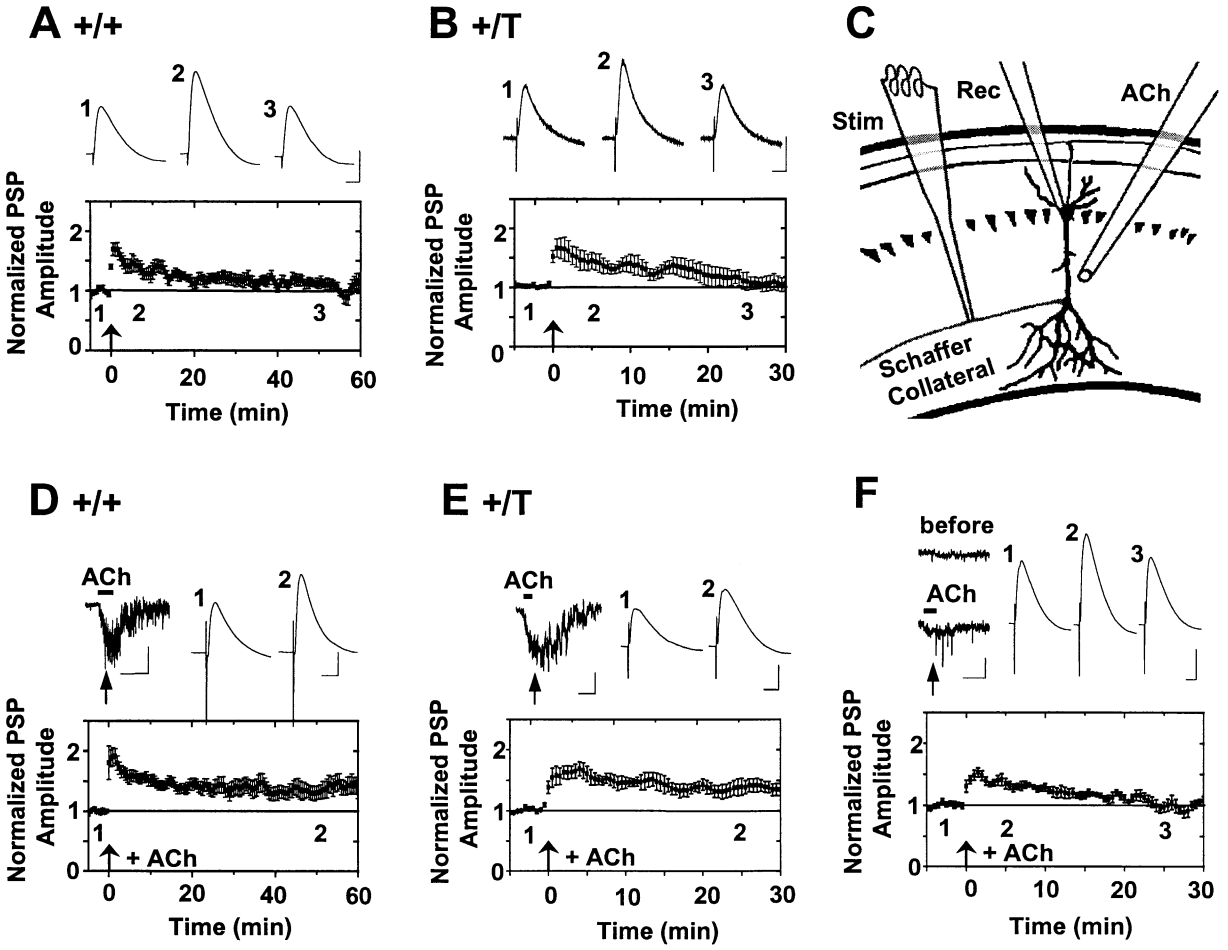

Figure 2. Postsynaptic Nicotinic Current in CA1 Pyramidal Neurons Boosts STP to LTP

(A) To produce reliable STP, the Schaffer collateral pathway was stimulated (1 s at 100 Hz) while depolarizing the current-clamped pyramidal neuron (1 s of 100 pA). Representative ePSPs are shown above at the times indicated in the average time course of the STP. The ↑ represents when the electrical stimulation was applied. The recordings were from (+/+) wild-type mice. For all the ePSP traces in this figure, the scale bars represent 20 ms and 5 mV.

(B) The same STP protocol was applied to α7 mutant mice (L250T). Representative ePSPs are shown at the times indicated in the average time course of the STP. The ↑ represents when the electrical stimulation was applied.

(C) Didactic diagram showing the arrangement of the recording pipette (Rec) on the CA1 pyramidal neuron, the ACh-puffer pipette (ACh), and the stimulating electrode (Stim).

(D) The first upper trace is postsynaptic nicotinic current recorded from the pyramidal neuron as a consequence of the ACh puff (horizontal bar). The ↑ represents the time when the electrical stimulation would be applied, just before the peak of the nicotinic current. For all the ACh-induced, voltage-clamped currents, the scale bars represent 2 s and 20 pA. Representative ePSPs are shown at the times indicated in the average time course of the STP. The recordings were from (+/+) wild-type mice.

(E) The same as (D), but the recordings were from α7 (+/T) mutant mice.

(F) Control experiments showing that small postsynaptic nAChRs are not sufficient to produce LTP with this electrical stimulation protocol. The first upper traces are the voltage-clamp records taken "before" and during the "ACh" puff onto the pyramidal neuron. The ↑ represents when the electrical stimulation would be applied. The next 3 traces are representative ePSPs taken at the times indicated on the average time course of the STP. The ↑ represents when the nicotinic current and the electrical stimulation were paired. Because it was unusual for +/T mice to have small ACh-induced currents, all the 7 cells in this group were taken from +/+ animals.

paradigm of electrical stimulation, 5 of the 7 cells tested underwent STP and 2 underwent LTP.

Nicotinic Currents in GABAergic Interneurons Inhibited Nearby Pyramidal Neurons

It has been shown previously that rat CA1 interneurons have relatively large nAChR currents (Frazier et al., 1998b; Jones and Yakel, 1997; McQuiston and Madison, 1999). We verified that finding for mutant mice (+/T) and their wild-type littermates (+/+). ACh-induced currents from CA1 interneurons were defined as measurable if they were >5 pA and the average current was 43.6 ± 12.8 pA, n = 6 out of 7 from (+/+) mice and 203.2 ± 47.5 pA, n = 10 out of 10 from (+/T) mutant mice.

We then tested that nAChR excitation of interneurons can cause inhibition of nearby pyramidal neurons (Alkondon et al., 2000; Ji and Dani, 2000). While recording from a CA1 pyramidal neuron, ACh was puffed onto a nearby GABAergic interneuron from a mutant mouse

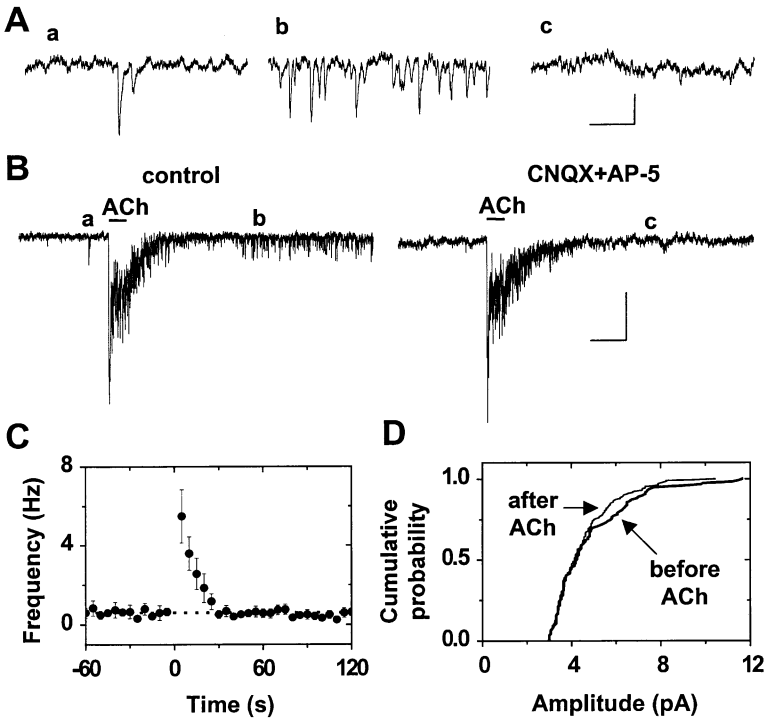

Figure 3. In a Minority of Cases, ACh Puffs into the Dendrites Enhances the mEPSC Frequency

(A) Examples of mEPSCs recorded in the presence of 0.5 μM TTX before (a) and just after (b) the ACh puff, as indicated in (B). Application of 25 μM CNQX and 50 μM AP-5 (c) prevented the glutamatergic mEPSCs. The scale bars represent 0.2 s and 5 pA.

(B) ACh-induced nicotinic currents recorded from a CA1 pyramidal cell are accompanied by an increase in mEPSCs that are inhibited in CNQX and AP-5. The scale bars represent 2 s and 20 pA.

(C) In the 7 out of 24 attempts where the ACh puff increased the mEPSC frequency, the frequency is averaged and plotted. The average baseline mEPSC frequency was 0.6 Hz, and 5 s after the ACh puff, the mEPSC frequency was 5 ± 1.

(D) The cumulative amplitude distribution of the mEPSCs is statistically the same before and after the ACh-puff based on the Kolmogorov-Smirnov test ($D = 0.1$; $p = 0.4$; $n = 7$).

(+/T) or a wild-type littermate (+/+) (Figure 5A). If the interneuron was connected to the pyramidal neuron, a burst of inhibitory outward synaptic current was measured from the pyramidal neuron (Figure 5B). Bicuculline (10 μM), a $GABA_A$ receptor inhibitor, blocked the outward, hyperpolarizing current ($n = 2$). Because pyramidal dendrites and the interneuron intermingle, the ACh puff aimed at the interneuron sometimes first activated nAChRs on the pyramidal neuron dendrites (causing a downward deflection). That inward nAChR current preceded the burst of GABAergic synaptic current and was revealed more clearly after applying bicuculline (Figure 5B, arrow). The nonspecific nAChR inhibitor, mecamylamine, blocked both ACh-induced currents ($n = 4$). The results indicate that ACh-induced nAChR activity excited the interneuron to fire action potentials that were detected as a burst of $GABA_A$ inhibitory synaptic current measured from the pyramidal neuron. This conclusion was verified because blocking action potentials with TTX prevented the ACh-induced GABAergic synaptic activity (Ji and Dani, 2000). It was difficult to find connected pairs of interneurons and pyramidal neurons. Out of 190 attempts, 21 connected pairs were found: 11 from (+/+) mice and 10 from (+/T) mice.

Nicotinic Currents in Interneurons Blocked STP and Diminished LTP

To determine whether ACh-induced GABAergic inhibition of pyramidal neurons could affect synaptic plasticity, we recorded from a pyramidal neuron while applying our standard STP stimulus protocol paired with an ACh puff onto an interneuron (Figure 6A). The pyramidal neuron was first voltage clamped to find a connected interneuron and to determine exactly when the electrical stimulation should be applied. The ACh puff aimed at the interneuron sometimes first activated nAChRs on the pyramidal neuron dendrites (Figure 6B, asterisk), then activated nAChRs on the interneuron causing inhibition at the pyramidal neuron (Figure 6B, upward arrow). The time course of the nAChR current was caused by the position of the ACh-puffer pipette relative to the interneuron soma and the intermingled pyramidal dendrites. If we had paired stimulation of the Schaffer collaterals with the excitatory nAChR currents in the pyramidal neuron (Figure 6B, asterisk), LTP would have been more likely, as found in Figure 2. Instead, when we delayed the standard STP stimulus protocol until the GABAergic inhibition reached the pyramidal neuron (Figure 6B, arrow), STP was prevented (Figure 6C). On average, none of the test ePSPs were significantly larger than baseline ($p > 0.05$). If there had been no ACh puffed onto the interneuron, STP would have been produced, as shown by the solid curve in Figure 6C. With this paradigm, 6 of the 8 cells tested showed no significant change, 1 underwent STP, and 1 underwent LTP.

Using the same recording arrangement (Figure 6A), the standard STP stimulus protocol was repeated three times (each separated by 20 s) to produce LTP consistently (Figure 7A). Seven of the 8 trials produced LTP. In separate experiments, the identical electrical stimulation was timed to arrive while the pyramidal neuron was inhibited by an ACh puff onto a nearby interneuron. Nicotinic excitation of the interneuron prevented LTP induction, and instead STP resulted (Figure 7B). The test ePSPs were no longer significantly larger than baseline ($p > 0.05$) 5 min after the stimulation. With this paradigm, 1 of the 7 cells tested showed no significant change, 4 underwent STP, and 2 underwent LTP of lesser magnitude than in the control. In separate experiments, we found that if the ACh application onto the interneuron

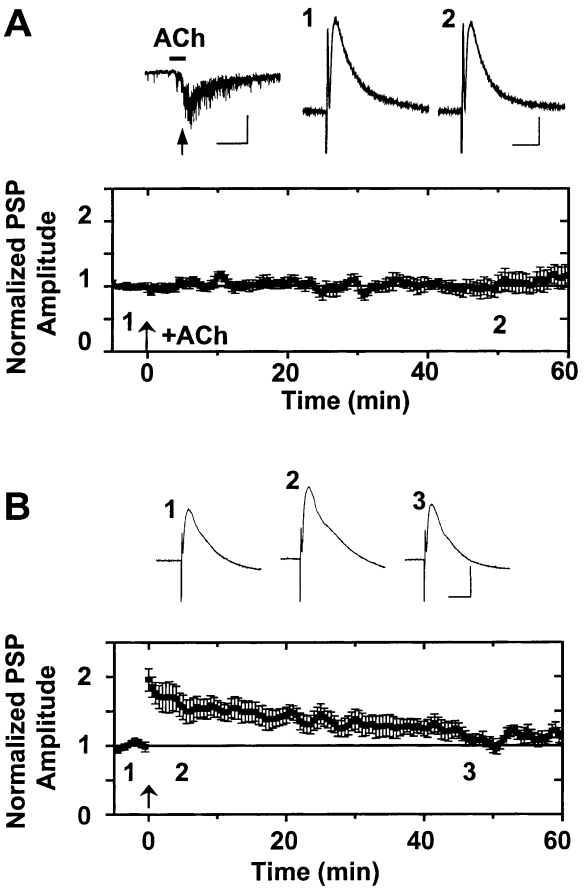

Figure 4. ACh-Induced Enhancement of Synaptic Plasticity Arises from Multiple Nicotinic Mechanisms

(A) When ACh-induced nAChR activity was paired with a postsynaptic depolarization (100 pA for 1 s) but without electrical stimulation of the Schaffer collaterals, there was not synaptic potentiation (on average). The first upper trace is postsynaptic nicotinic current recorded from the pyramidal neuron as a consequence of the ACh puff (horizontal bar). The ↑ represents when the postsynaptic depolarization would be applied. The next 2 traces are representative ePSPs, as indicated on the average time course. The ↑ represents when the stimulus protocol was applied. The recordings were from (+/+) wild-type mice. The scale bars represent 2 s and 20 pA under voltage clamp, and 20 ms and 2 mV under current clamp.

(B) When the postsynaptic depolarizing current was doubled (200 pA for 1 s), longer-lasting STP was produced, but LTP was not produced (on average). In this case, the postsynaptic depolarization was paired with stimulation of the Schaffer collaterals (100 Hz for 1 s), but there was no ACh puff applied.

did not produce inhibition of the pyramidal neuron, then there was no effect on LTP induction (n = 7, data not shown).

Discussion

There has been some controversy about the presence of nAChRs on pyramidal neurons (Frazier et al., 1998b; Hefft et al., 1999; Jones and Yakel, 1997; McQuiston and Madison, 1999). We directly addressed that issue by measuring ACh-induced currents from CA1 pyramidal neurons. Depending on the position of the ACh-puffer pipette, we were able to detect nicotinic currents in most of the CA1 pyramidal neurons from wild-type (+/+) mice. The result was confirmed in heterozygous littermate mice with the L250T mutation in the α7 subunit, (+/T). That mutation effectively increases the α7* ACh-induced currents by greatly reducing the nonconducting desensitized state (Revah et al., 1991; Bertrand et al., 1992). Previous and ongoing work indicates that the expression of α7* nAChRs in +/T mice is similar to the expression in the +/+ mice, and there have been no detectable compensatory changes in other nAChR subunits (Orr-Urtreger et al., 2000). Because the α7* subtype of nicotinic receptor predominates in the rodent hippocampus (Alkondon and Albuquerque, 1993; Gray et al., 1996; Jones and Yakel, 1997; Frazier et al., 1998a, 1998b; McQuiston and Madison, 1999), much larger currents were measured from the mutant (+/T) mice, revealing that more than 90% of the CA1 pyramidal neurons have significant nAChR expression.

Under some circumstances, the expression of nAChRs on pyramidal neurons was sufficient to influence synaptic plasticity. Postsynaptic nAChR activity on a pyramidal neuron boosted the impact of a weak electrical stimulation of the Schaffer collateral pathway, causing the production of LTP. A stimulation paradigm that normally produced STP was boosted to produce LTP only when a sufficiently large postsynaptic nicotinic current was induced at the correct time. The nicotinic current was timed to coincide with the electrical stimulation. In that way, the postsynaptic depolarization caused by the nicotinic current arrived at the correct moment to add onto the postsynaptic glutamatergic currents. The added depolarization caused by the nAChR activity would help to relieve the Mg^{2+} block of the NMDA receptor, setting in motion the calcium-dependent cascade and electrical events leading to LTP (Malenka and Nicoll, 1999; Martin et al., 2000).

An increased postsynaptic depolarization does not explain all the success of the nAChR activity. When we simply doubled the postsynaptic depolarization paired to the electrical stimulation of the Schaffer collaterals, we did not consistently produce LTP, as was seen with the ACh-induced effect. Properly timed nicotinic currents also would contribute to the postsynaptic calcium signal mediated by NMDA receptors. The hippocampal nicotinic currents were predominantly mediated by α7* nAChRs, which have a high-calcium permeability (Séguéla et al., 1993; Castro and Albuquerque, 1995). Furthermore, the nAChRs are not blocked at negative potentials by Mg^{2+}, as are the NMDA receptors. Therefore, at the resting potential near −70 mV, there was a strong voltage driving force for Ca^{2+} to enter the postsynaptic pyramidal neuron through the active nAChRs. Consequently, active postsynaptic nAChRs mediated a depolarizing current partially carried by Ca^{2+}, summing with the depolarization and Ca^{2+} signal mediated by glutamate receptors and boosting the induction of LTP.

A third way in which nAChR activity increased the probability of producing LTP was via presynaptic nAChRs. Activation of presynaptic nAChRs (when present) enhanced the synaptic release of glutamate, as we showed with the increased mEPSC frequency. This effect has been shown many times in many different areas of the mammalian brain (Albuquerque et al., 1997; Alkondon et al., 1996, 1997a; Aramakis and Metherate, 1998; Gray

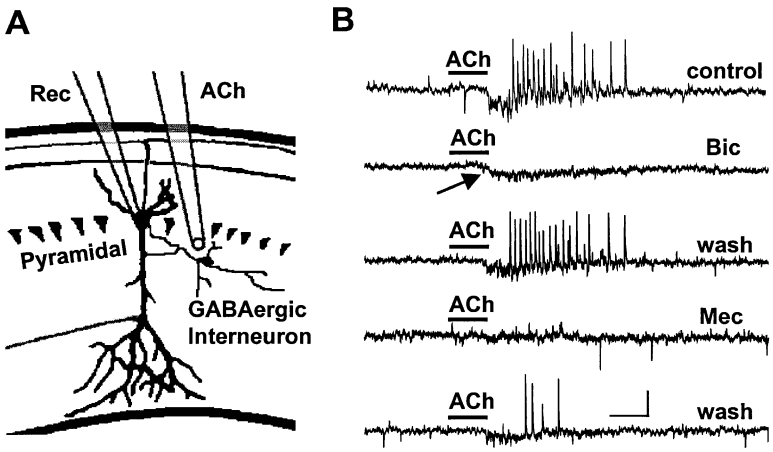

Figure 5. ACh Application onto CA1 Interneurons Produced GABAergic Inhibition of a Nearby Pyramidal Neuron

(A) Didactic diagram showing the arrangement of the recording pipette (Rec) on the pyramidal neuron, and the ACh-puffer pipette (ACh) aimed toward the soma of the interneuron.

(B) Current traces recorded from a pyramidal neuron are shown for an ACh application (control), with inhibition of $GABA_A$ receptors with 10 μM bicuculline (Bic), and after recovery of the $GABA_A$ synaptic activity (15 min wash). In the same cell, inhibition of the nAChRs by 5 μM mecamylamine (Mec) prevents both phases of the currents, and there is partial recovery (60 min wash). The arrow on the Bic trace indicates nAChR current activated directly on the postsynaptic CA1 pyramidal neuron dendrites. In 8 of the 21 pairs, the ACh puff induced biphasic currents, but in the other 13 cases only the GABAergic synaptic currents were seen. The scale bars represent 1 s and 20 pA.

et al., 1996; Jones et al., 1999; McGehee et al., 1995; McGehee and Role, 1995; Radcliffe and Dani, 1998; Wonnacott, 1997). By increasing the synaptic release of glutamate, properly timed nAChR activity increased the coincidence between presynaptic release and postsynaptic depolarization, enhancing the probability of LTP. This form of nicotinic presynaptic modulation has been clearly demonstrated by Mansvelder and McGehee (2000) in the ventral tegmental area. Under our experimental conditions, this form of modulation was seen less frequently, affecting only 10%–15% of our trials.

Nicotinic currents also were able to act indirectly to diminish or prevent the induction of synaptic plasticity. It has been shown previously that nAChRs are more highly expressed on rat GABAergic interneurons than on pyramidal neurons (Frazier et al., 1998b; Hefft et al.,

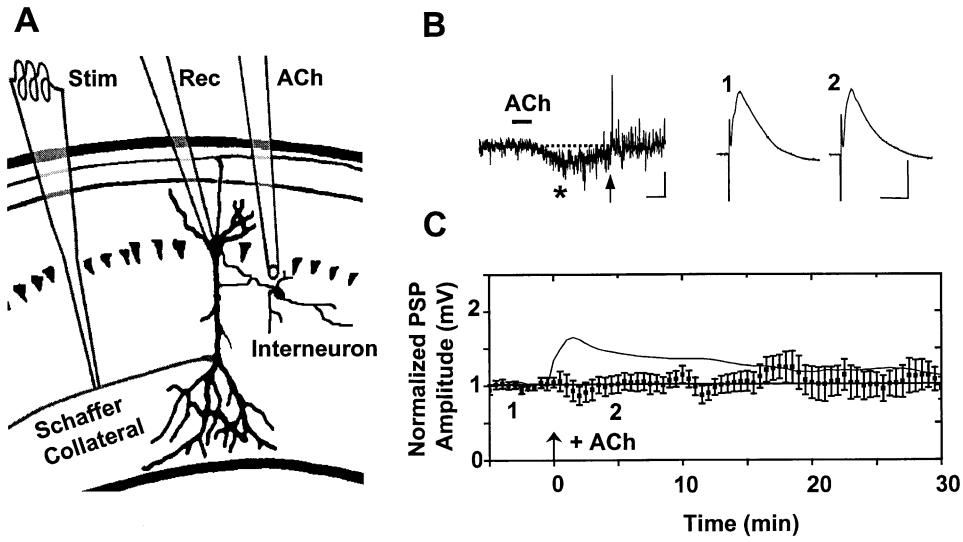

Figure 6. ACh-Induced GABAergic Synaptic Activity Blocks the Induction of STP

(A) Didactic diagram showing the arrangement of the recording pipette (Rec), the ACh-puffer pipette (ACh), and the stimulating electrode (Stim).

(B) The first trace is the pyramidal neuron's response activated by the ACh puff (horizontal bar) aimed toward the soma of the interneuron. Because pyramidal neuron dendrites intermingle near the interneuron, the ACh puff produced a biphasic current recorded from the pyramidal neuron. The initial inward current (*) arises from the direct activation of nAChRs on the pyramidal neuron's dendrites. The later rapid upward deflections are the GABAergic synaptic currents activated by nAChRs on the interneuron. The ↑ represents when the electrical stimulation would be applied during the GABAergic inhibition of the pyramidal neuron. The scale bars represent 1 s and 10 pA. The next 2 traces are representative ePSPs taken as indicated in (C). The scale bars represent 50 ms and 2 mV.

(C) The average time course of the ePSPs is shown, and ↑ represents when the GABAergic inhibition and the electrical stimulation were paired. The smooth solid line represents the STP that normally resulted from the stimulation paradigm without the ACh pairing (taken from Figures 2A, 2B, and 2F). Out of the 8 cells included in the analysis, 5 were taken from the +/T mice, and 3 were from the +/+ littermate mice.

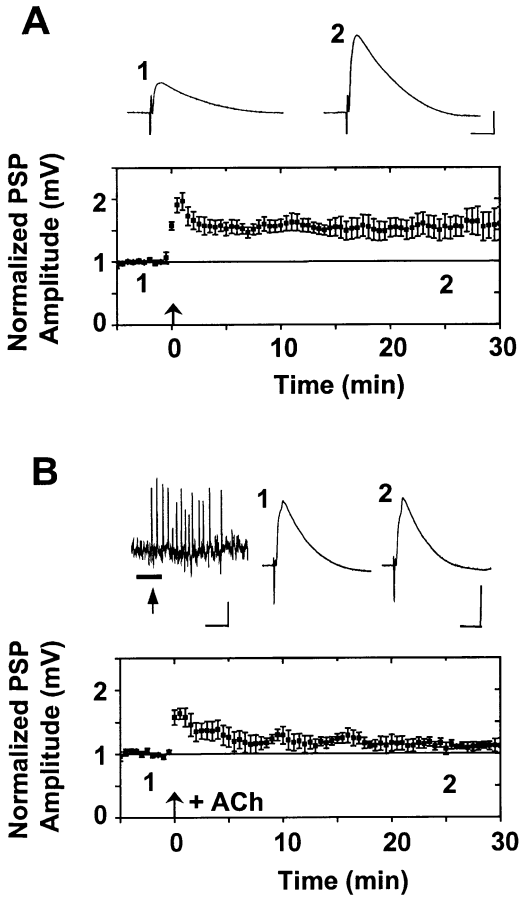

Figure 7. ACh-Induced GABAergic Synaptic Activity Suppresses the Induction of LTP, Resulting in STP

(A) To produce reliable LTP, the Schaffer collateral pathway was stimulated (3 times for 1 s at 100 Hz) while depolarizing the current-clamped pyramidal neuron (3 times for 1 s with 100 pA depolarizing current). The 2 upper traces are representative ePSPs at the baseline (1) and at 25 min (2) after the electrical stimulation (↑) that induced LTP. The scale bars represent 50 ms horizontally and 2 mV vertically. The average time course of the LTP is shown below, and ↑ represents when the electrical stimulation was applied. Out of the 8 cells included in the analysis, 4 were taken from the +/T mice, and 4 were from the +/+ littermate mice.

(B) The first upper trace is the pyramidal neuron's response activated by the ACh puff (horizontal bar) aimed toward the soma of the interneuron. The upward deflections are the GABAergic synaptic currents activated by nAChRs on the interneuron. The ↑ represents the time when the electrical stimulation would be applied, during the GABAergic inhibition of the pyramidal neuron. The scale bars represent 1 s horizontally and 10 pA vertically. The next 2 traces are representative ePSPs at the baseline (1) and at 25 min (2) after the electrical stimulation (↑). The scale bars represent 50 ms horizontally and 2 mV vertically. The average time course of the ePSPs is shown below, and ↑ represents when the GABAergic inhibition and the electrical stimulation were paired. Out of the 7 cells included in the analysis, 4 were taken from the +/T mice, and 3 were from the +/+ littermate mice.

1999; Jones and Yakel, 1997; McQuiston and Madison, 1999; Ji and Dani, 2000), and we verified that finding in mice. Nicotinic currents activated by an ACh puff onto the soma usually excited the interneuron, causing it to fire action potentials that could be recorded from a nearby, connected pyramidal neuron as inhibitory $GABA_A$ receptor synaptic currents. When the ACh-induced GABAergic inhibition of the pyramidal neuron was properly timed to arrive just before and during electrical stimulation of the Schaffer collateral pathway, it strongly decreased the probability of observing synaptic plasticity. An electrical stimulation that normally produced STP had no effect when the electrical stimulation was paired with ACh-induced GABAergic inhibition of the pyramidal neuron. A stronger stimulation paradigm that normally produced LTP was diminished by the ACh-induced GABAergic inhibition so that only STP resulted. Because the inhibition of the pyramidal neuron was timed to arrive before and during the electrical stimulation, the glutamatergic synaptic activity was prevented from causing a sufficient postsynaptic depolarization of the pyramidal neuron, and in that way synaptic potentiation was prevented or suppressed (Staley and Mody, 1992).

Importance of the Location and Timing of nAChR Activity

Nicotinic receptors can be located presynaptically, postsynaptically, and nonsynaptically, for instance, at the soma. This study indicates that nAChRs at presynaptic locations or on excitatory neurons can enhance or cause synaptic change by three different mechanisms. Presynaptic nAChRs can enhance release, and postsynaptic receptors can add to the postsynaptic depolarization and calcium signal. Properly timed, all three of those mechanisms will strengthen the coincidence of presynaptic and postsynaptic activity and boost synaptic potentiation. It is not hard to imagine, however, nAChR activity that is timed to miss synaptic coincidence, helping to create synaptic depression. For example, postsynaptic nAChR activity could produce a depolarization and calcium signal that precedes the presynaptic action potential. Such a situation would favor synaptic depression, not potentiation.

Because nAChRs are more highly expressed on GABAergic interneurons, they are more likely to play a greater role by influencing inhibitory activity. There are many GABAergic neurons participating in the hippocampal slice, and we did not inhibit GABAergic interneurons during the electrical induction of LTP. An interesting aspects of our results is that despite the participation of a large number of interneurons during the electrical stimulation paradigm, the nicotinic activation of basically one selected interneuron was sufficient to tip the balance against LTP. In this case, the particular interneuron had inhibitory impact, but other interneurons can cause disinhibition (Ji and Dani, 2000), which would favor the induction of LTP for other pyramidal neurons. Thus, there is the potential for local modulation of synaptic plasticity by nAChRs, allowing a particular neuron or a particular synapse to respond differently than the average of the surrounding circuitry.

Although there is the potential for specific local control, interneurons may also influence the overall hippocampal activity by regulating the rhythmic patterns associated with various states of the animal. During exploratory behavior and paradoxical sleep (REM), theta rhythms become the predominant hippocampal firing pattern (Klimesch, 1999). Those rhythmic patterns arise from network coherence, and GABAergic interneurons

are critical elements that synchronize the principal cells (Wang and Buzsaki, 1996). Rhythmic firing from GABAergic and cholinergic neurons in the medial septum/diagonal band complex modulates the theta rhythms (Brazhnik and Fox, 1997). Depending on the phase within the theta cycle, different forms of synaptic plasticity are favored. At the peak of the theta cycle, LTP is favored. Again, timing is vital, and nAChRs are likely to participate in the overall process.

The broader importance of nAChR activity extends beyond the immediate effect at specific synapses. Cholinergic varicosities in the hippocampus do not always match with synaptic specializations, indicating that the majority of cholinergic release may be via diffuse, volume transmission (Umbriaco et al., 1995). In that case, broad changes in the concentration of ACh or choline (Papke et al., 1996; Alkondon et al., 1997b) could activate nAChRs on the soma or at other nonsynaptic locations. The resulting depolarization and intracellular calcium signal could modify the basic set point of the cell, making it more or less able to participate in subsequent neuronal events.

Conclusion

The main finding is that nicotinic cholinergic activity can potently alter the induction of synaptic plasticity that processes via standardly accepted mechanisms. Depending on the distributions of various nAChR subtypes and the timing of nAChR activity, cellular and synaptic events can be modified in many different ways. Presynaptic nAChRs can increase the probability of neurotransmitter release, increasing the fidelity of synaptic transmission. Postsynaptic nAChRs can increase the depolarization and calcium signal associated with successful transmission, helping to initiate intracellular cascades. On the other hand, nicotinic activity can have potent impact upon interneuron activity, regulating the excitability of circuits. The location of nAChR activity and the moment-by-moment change in that activity can tip the balance in favor or against the induction of synaptic plasticity. The expansive, diffuse innervation by the cholinergic system and the diverse array of nicotinic mechanisms ensures that nAChR activity participates in broad-based computations throughout the CNS. Thus, it is not surprising that nicotinic mechanisms have been implicated in learning, memory, and attention, as well as sleep cycle disorders, analgesia, Tourette's syndrome, and epilepsy. During Alzheimer's disease, there is a loss of nAChRs and cholinergic projections associated with declining cognitive functions. Mechanisms like the ones indicated here are likely to contribute to the influences of nAChRs within the mammalian central nervous system.

Experimental Procedures

Hippocampal Slice and Electrophysiology

Most of the experiments were performed using young mice (14–24 days) born from N6 breeding pairs of the genotype (+/+) and (+/T) for the α7 subunit (Orr-Urtreger et al., 2000). The mice were used prior to genotyping. In early experiments, a few wild-type C57BL mice were used. Animals were anesthetized with halothane and were decapitated. Horizontal slices 300 μm thick were cut in ice-cold cutting solution (in mM): 220 sucrose, 2.5 KCl, 30 $NaHCO_3$, 1.25 NaH_2PO_4, 10 dextrose, 7 $MgCl_2$, and 1 $CaCl_2$, bubbled with 95% O_2 and 5% CO_2. Slices were transferred into a holding chamber, containing the external solution (in mM): 125 NaCl, 2.5 KCl, 25 $NaHCO_3$, 1.25 NaH_2PO_4, 25 dextrose, 1 $MgCl_2$, and 2 $CaCl_2$, oxygenated with 95% O_2 and 5% CO_2. After a 30 min recovery at 35°C, slices were maintained at room temperature and were used for recording in the following 5 hr.

All the electrophysiological recordings were obtained at 32°C–34°C, and 1 μM atropine always inhibited muscarinic acetylcholine receptors. The whole-cell patch-clamp configuration was used in either voltage-clamp or current-clamp mode. The recording pipettes were filled with the following solution (in mM): 130 K-gluconate, 4 KCl, 10 *N*-2-hydroxyethylpiperazine-*N*′-2-ethanesulfonic acid, 0.2 ethylene glycol-bis (β-aminoethyl ether) *N*, *N*, *N*′, *N*′-tetraacetic acid (EGTA), 4 ATP (magnesium salt), 0.3 GTP (sodium salt), and 7 phosphocreatine, adjusted to pH 7.3–7.4 with KOH. The recording pipettes had resistances of 3–6 MΩ. Neurons were visualized by DIC microscopy. Data were acquired with an Axopatch amplifier at 10 kHz and stored on a hard drive. Series resistance and input resistance were monitored by injecting a small negative voltage or current step regularly throughout the experiment. Series resistance was usually in a range of 5–30 MΩ and was left uncompensated. Data were discarded if series or input resistance changed by 30% or more.

When antagonists (MLA, mecamylamine, CNQX, AP-5, and bicuculline) were used, they were applied via bath perfusion at about 3 ml/min. The agonist, 1 mM ACh, was prepared each day.

Stimulation, Recording Sites, and Synaptic Plasticity

To record ACh-induced currents from a CA1 pyramidal neuron, a pressure-injection pipette (puffer) was used to deliver the agonist; and a Picospritzer (Parker Instrument) was used to control the pressure and duration of the puff. The puffer pipettes had resistances of about 4 MΩ. In all of the experiments, a 1 s puff with 5–10 psi was used. One position of the ACh-puffer pipette was pointed toward the dendrites 50–100 μm distal and about 50 μm lateral of the soma (ACh 1; Figure 1A). The puffer pipette was aimed mostly perpendicular to the dendrites. In other experiments, the puffer was located in the distal dendrites roughly 200–300 μm from the soma (ACh 2; Figure 1A) and was aimed more parallel to the dendrites, but was not aimed directly at the soma. In this position, larger currents were produced because a greater surface area of dendrites was hit by the ACh puff. To record ACh-induced GABAergic currents from a pyramidal neuron, an ACh-puffer pipette was pointed toward the soma of a nearby interneuron in the stratum radiatum (Figure 5A). The puffer pipette was positioned $\geq$100 μm from the soma of the pyramidal neuron to minimize the inadvertent activation of nAChRs on the dendrites of the pyramidal neuron.

A bipolar electrode was used to stimulate the Schaffer collateral inputs to a pyramidal neuron to induce STP or LTP. Evoked postsynaptic potentials (ePSPs) were triggered by a 100 μs stimulus and were recorded every 30 s. The stimulation intensity was adjusted to evoke a 6–10 mV ePSP, and the intensity was usually 20–70 μA. The electrode was a glass pipette painted with conductive silver paint and filled with the external solution. The tip of the stimulating electrode was placed in the stratum radiatum 50–250 μm lateral from the recording pipette on the soma of the pyramidal neuron (Figure 2C). STP was induced by a 1 s train of 100 Hz delivered through the stimulating electrode, paired with a 1 s depolarizing current (100 pA) injected through the patch pipette into the current-clamped pyramidal neuron. For the experiments in Figure 7, LTP was induced by repeating the STP paradigm three times each separated by 20 s. When treating with ACh (Figure 7B), we applied ACh prior to each of the three stimulus trains.

To study the effect of nAChR activity on the induction of STP or LTP, we first had to determine the amplitude and timing of the ACh-induced currents measured from the pyramidal neuron of interest. Therefore, we voltage-clamped a pyramidal neuron at $-$60 mV and evaluated the amplitude and the onset of the ACh-induced nicotinic currents directly from that pyramidal neuron. Then the recording was switched to current-clamp mode to begin the electrical stimulation paradigm. On the other hand, before studying the GABAergic inhibition, it was necessary to find a nearby interneuron that was connected to the voltage-clamped CA1 pyramidal neuron. The amplitude, onset, and duration of the hyperpolarizing GABAergic synaptic

currents induced by the ACh puff were evaluated. For these experiments, we selected pyramidal neurons that showed a GABAergic response of 5 Hz or more. Then the recording was switched to current-clamp mode, and the electrical stimulation was applied after carefully testing and adjusting the stimulating electrode to be more than 300 μm from the ACh puffer to avoid direct electrical stimulation of that particular interneuron (Figure 6A). While in current clamp, the membrane potential was manually adjusted to -72 ± 2 mV.

After recording a stable ePSP baseline for 5 min or more, the electrical stimulation was applied to induce STP or LTP. That stimulation was properly timed by computer to coincide with nAChR activity induced by an ACh puff onto either the pyramidal neuron's dendrites or onto the soma of the selected nearby interneuron. When we examined the effect caused by direct nAChR depolarization of the pyramidal neuron, the electrical stimulation was delivered about 200 ms before the peak of the nicotinic currents. When examining the effect of ACh-induced GABAergic inhibition, the electrical stimulation was delivered about 200 ms after the onset time of the GABAergic synaptic burst. The recordings were continued as long as the whole-cell seal remained stable and the series resistance did not change.

The following procedures were used for analysis and display purposes. All of the ePSPs amplitudes during the 5 min prior to the electrical stimulation were averaged to determine the baseline for normalization in the STP and LTP experiments. For each stimulation paradigm, all of the results were averaged no matter what outcome was obtained, and the displayed ePSPs were the average of 3–5 traces. These amplitudes were compared to the average baseline amplitude using the Student's t test. For display, the averaged time course applied a running average of three points. Currents were sometimes additionally filtered offline for presentation.

Acknowledgments

We thank A. Orr-Urtreger and A.L. Beaudet for providing the mutant mice and F.-M. Zhou for commenting on the manuscript. The National Institute of Neurological Disorders and Stroke (NS21229) and the National Institute on Drug Abuse (DA09411 and DA12661) supported this work.

Received November 21, 2000; revised April 23, 2001.

References

Albuquerque, E.X., Alkondon, M., Pereira, E.F., Castro, N.G., Schrattenholz, A., Barbosa, C.T., Bonfante-Cabarcas, R., Aracava, Y., Eisenberg, H.M., and Maelicke, A. (1997). Properties of neuronal nicotinic acetylcholine receptors: pharmacological characterization and modulation of synaptic function. J. Pharmacol. Exp. Ther. *280*, 1117–1136.

Alkondon, M., and Albuquerque, E.X. (1993). Diversity of nicotinic acetylcholine receptors in rat hippocampal neurons. I. Pharmacological and functional evidence for distinct structural subtypes. J. Pharmacol. Exp. Ther. *265*, 1455–1473.

Alkondon, M., Pereira, E.F., Barbosa, C.T.F., and Albuquerque, E.X. (1997a). Neuronal nicotinic acetylcholine receptor activation modulates gamma-aminobutyric acid release from CA1 neurons of rat hippocampal slices. J. Pharmacol. Exp. Ther. *283*, 1396–1411.

Alkondon, M., Pereira, E.F., Cortes, W.S., Maelicke, A., and Albuquerque, E.X. (1997b). Choline is a selective agonist of alpha7 nicotinic acetylcholine receptors in the rat brain neurons. Eur. J. Neurosci. *9*, 2734–2742.

Alkondon, M., Rocham, E.S., Maelicke, A., and Albuquerque, E.X. (1996). Diversity of nicotinic acetylcholine receptors in rat brain. V. alpha-Bungarotoxin-sensitive nicotinic receptors in olfactory bulb neurons and presynaptic modulation of glutamate release. J. Pharmacol. Exp. Ther. *278*, 1460–1471.

Alkondon, M., Pereira, E.F., and Albuquerque, E.X. (1998). Alpha-bungarotoxin- and methyllycaconitine-sensitive nicotinic receptors mediate fast synaptic transmission in interneurons of rat hippocampal slices. Brain Res. *810*, 257–263.

Alkondon, M., Pereira, E.F., Eisenberg, H.M., and Albuquerque, E.X. (2000). Nicotinic receptor activation in human cerebral cortical interneurons: a mechanism for inhibition and disinhibition of neuronal networks. J. Neurosci. *20*, 66–75.

Aramakis, V.B., and Metherate, R. (1998). Nicotine selectively enhances NMDA receptor-mediated synaptic transmission during postnatal development in sensory neocortex. J. Neurosci. *18*, 8485–8495.

Bertrand, D., Devillers-Thiery, A., Revah, F., Galzi, J.L., Hussy, N., Mulle, C., Bertrand, S., Ballivet, M., and Changeux, J.P. (1992). Unconventional pharmacology of a neuronal nicotinic receptor mutated in the channel domain. Proc. Natl. Acad. Sci. USA *89*, 1261–1265.

Brazhnik, E.S., and Fox, S.E. (1997). Intracellular recordings from medial septal neurons during hippocampal theta rhythm. Exp. Brain Res. *114*, 442–453.

Brioni, J.D., and Arneric, S.P. (1993). Nicotinic receptor agonists facilitate retention of avoidance training: participation of dopaminergic mechanisms. Behav. Neural Biol. *59*, 57–62.

Buccafusco, J.J., Jackson, W.J., Terry, A.V., Jr., Marsh, K.C., Decker, M.W., and Arneric, S.P. (1995). Improvement in performance of a delayed matching-to-sample task by monkeys following ABT-418: a novel cholinergic channel activator for memory enhancement. Psychopharmacology (Berl.) *120*, 256–266.

Castro, N.G., and Albuquerque, E.X. (1995). Alpha-bungarotoxin-sensitive hippocampal nicotinic receptor channel has a high calcium permeability. Biophys. J. *68*, 516–524.

Coggan, J.S., Paysan, J., Conroy, W.G., and Berg, D.K. (1997). Direct recording of nicotinic responses in presynaptic nerve terminals. J. Neurosci. *17*, 5798–5806.

Frazier, C.J., Buhler, A.V., Weiner, J.L., and Dunwiddie, T.V. (1998a). Synaptic potentials mediated via α-bungarotoxin-sensitive nicotinic acetylcholine receptors in rat hippocampal interneurons. J. Neurosci. *18*, 8228–8235.

Frazier, C.J., Rollins, Y.D., Breese, C.R., Leonard, S., Freedman, R., and Dunwiddie, T.V. (1998b). Acetylcholine activate an α-bungarotoxin-sensitive nicotinic current in rat hippocampal interneurons, but not pyramidal cells. J. Neurosci. *18*, 1187–1195.

Frotscher, M., and Leranth, C. (1985). Cholinergic innervation of the rat hippocampus as revealed by choline acetyltransferase immunocytochemistry: a combined light and electron microscopic study. J. Comp. Neurol. *239*, 237–246.

Fujii, S., Ji, Z., Morita, N., and Sumikawa, K. (1999). Acute and chronic nicotine exposure differentially facilitate the induction of LTP. Brain Res. *846*, 137–143.

Girod, R., Barazangi, N., McGehee, D., and Role, L.W. (2000). Facilitation of glutamatergic neurotransmission by presynaptic nicotinic acetylcholine receptors. Neuropharmacology *39*, 2715–2725.

Gray, R., Rajan, A.S., Radcliffe, K.A., Yakehiro, M., and Dani, J.A. (1996). Hippocampal synaptic transmission enhanced by low concentrations of nicotine. Nature *83*, 713–716.

Grigoryan, G.A., Mitchell, S.N., Hodges, H., Sinden, J.D., and Gray, J.A. (1994). Are the cognitive-enhancing effects of nicotine in the rat with lesions to the forebrain cholinergic projection system mediated by an interaction with the noradrenergic system? Pharmacol. Biochem. Behav. *49*, 511–521.

Hamid, S., Dawe, G.S., Gray, J.A., and Stephenson, J.D. (1997). Nicotine induces long-lasting potentiation in the dentate gyrus of nicotine-primed rats. Neurosci. Res. *29*, 81–85.

Hefft, S., Hulo, S., Bertrand, D., and Muller, D. (1999). Synaptic transmission at nicotinic acetylcholine receptors in rat hippocampal organotypic cultures and slices. J. Physiol. (Lond.) *515*, 769–776.

Ji, D., and Dani, J.A. (2000). Inhibition and disinhibition of pyramidal neurons by activation of nicotinic receptors on hippocampal interneurons. J. Neurophysiol. *83*, 2682–2690.

Jones, S., Sudweeks, S., and Yakel, J.L. (1999). Nicotinic receptors in the brain: correlating physiology with function. Trends Neurosci. *22*, 555–561.

Jones, S., and Yakel, J.L. (1997). Functional nicotinic ACh receptors on interneurons in the rat hippocampus. J. Physiol. *504*, 603–610.

Klimesch, W. (1999). EEG alpha and theta oscillations reflect cogni-

tive and memory performance: a review and analysis. Brain. Res. Brain. Res. Rev. *29*, 169–195.

Lena, C., and Changeux, J.P. (1997). Role of Ca^{2+} ions in nicotinic facilitation of GABA release in mouse thalamus. J. Neurosci. *17*, 576–585.

Levin, E.D., and Simon, B.B. (1998). Nicotinic acetylcholine involvement in cognitive function in animals. Psychopharmacology *138*, 217–230.

Levin, E.D., and Rezvani, A.H. (2000). Development of nicotinic drug therapy for cognitive disorders. Eur. J. Pharmacol. *393*, 141–146.

Malenka, R.C., and Nicoll, R.A. (1999). Long-term potentiation—a decade of progress? Science *285*, 1870–1874.

Mansvelder, H.D., and McGehee, D.S. (2000). Long-term potentiation of excitatory inputs to brain reward areas by nicotine. Neuron *27*, 349–357.

Martin, S.J., Grimwood, P.D., and Morris, R.G. (2000). Synaptic plasticity and memory: an evaluation of the hypothesis. Annu. Rev. Neurosci. *23*, 649–711.

McGehee, D.S., and Role, L.W. (1995). Physiological diversity of nicotinic acetylcholine receptors expressed by vertebrate neurons. Annu. Rev. Physiol. *57*, 521–546.

McGehee, D.S., Heath, M.J., Gelber, S., Devay, P., and Role, L.W. (1995). Nicotine enhancement of fast excitatory synaptic transmission in CNS by presynaptic receptors. Science *269*, 1692–1696.

McQuiston, A.R., and Madison, D.V. (1999). Nicotinic receptor activation excites distinct subtypes of interneurons in the rat hippocampus. J. Neurosci. *19*, 2887–2896.

Newhouse, P.A., Potter, A., and Levin, E.D. (1997). Nicotinic system involvement in Alzheimer's and Parkinson's diseases. Implications for therapeutics. Drugs Aging *11*, 206–228.

Ohno, M., Yamamoto, T., and Watanabe, S. (1993). Blockade of hippocampal nicotinic receptors impairs working memory but not reference memory in rats. Pharmacol. Biochem. Behav. *45*, 89–93.

Orr-Urtreger, A., Broide, R.S., Kasten, M.R., Dang, H., Dani, J.A., Beaudet, A.L., and Patrick, J.W. (2000). Mice homozygous for the L250T mutation in the alpha7 nicotinic acetylcholine receptor show increased neuronal apoptosis and die within 1 day of birth. J. Neurochem. *74*, 2154–2166.

Papke, R.L., Bencherif, M., and Lippiello, P. (1996). An evaluation of neuronal nicotinic acetylcholine receptor activation by quaternary nitrogen compounds indicates that choline is selective for the alpha 7 subtype. Neurosci. Lett. *213*, 201–204.

Paterson, D., and Nordberg, A. (2000). Neuronal nicotinic receptors in the human brain. Prog. Neurobiol. *61*, 75–111.

Revah, F., Bertrand, D., Galzi, J.L., Devillers-Thiery, A., Mulle, C., Hussy, N., Bertrand, S., Ballivet, M., and Changeux, J.P. (1991). Mutations in the channel domain alter desensitization of a neuronal nicotinic receptor. Nature *353*, 846–849.

Radcliffe, K., and Dani, J.A. (1998). Nicotinic stimulation produces multiple forms of glutamatergic synaptic enhancement. J. Neurosci. *18*, 7075–7083.

Séguéla, P., Wadiche, J., Dineley-Miller, K., Dani, J.A., and Patrick, J.W. (1993). Molecular cloning, functional properties, and distribution of rat brain α7: a nicotinic cation channel highly permeable to calcium. J. Neurosci. *13*, 596–604.

Staley, K.J., and Mody, I. (1992). Shunting of excitatory input to dentate gyrus granule cells by a depolarizing $GABA_A$ receptor-mediated postsynaptic conductance. J. Neurophysiol. *68*, 197–212.

Umbriaco, D., Garcia, S., Beaulieu, C., and Descarries, L. (1995). Relational features of acetylcholine, noradrenaline, serotonin and GABA axon terminals in the stratum radiatum of adult rat hippocampus (CA1). Hippocampus *5*, 605–620.

Wada, E., Wada, K., Boulter, J., Deneris, E., Heinemann, S., Patrick, J., and Swanson, L.W. (1989). Distribution of α2, α3, α4 and β2 neuronal nicotinic receptor subunit mRNAs in the central nervous system: a hybridization histochemical study in the rat. J. Comp. Neurol. *284*, 314–335.

Wang, X.J., and Buzsaki, G. (1996). Gamma oscillation by synaptic inhibition in a hippocampal interneuronal network model. J. Neurosci. *16*, 6402–6413.

Wonnacott, S. (1997). Presynaptic nicotinic ACh receptors. Trends Neurosci. *20*, 92–98.

Woolf, N.J. (1991). Cholinergic systems in mammalian brain and spinal cord. Prog. Neurobiol. *37*, 475–524.